A High Density Thin layer confining the H II region M 42. HHT measurements[0]

A. Rodríguez−Franco[1 2]

Departamento de Matemática Aplicada (Biomatemática), Sección departamental de Optica, Escuela Universitaria de Optica. Universidad Complutense de Madrid. Av. Arcos de Jalón s/n. E-28037 Madrid. Spain

T.L.Wilson [3]

MPIFR, Postfach 2024, D-53010 Bonn, Germany

J. Martín−Pintado, and A. Fuente

Observatorio Astronómico Nacional (IGN), Campus Universitario, Apdo. 1143, E-28800, Alcalá de Henares, Spain

Received ______________________; accepted ______________________

[0]This work is based on measurements made with the Heinrich Hertz Telescope, which is operated by the Submillimeter Telescope Observatory on behalf of Steward Observatory and the Max-Planck-Institut für Radioastronomie.

[1]Observatorio Astronómico Nacional (IGN), Campus Universitario, Apdo. 1143, E-28800, Alcalá de Henares, Spain.

[2]Present address: LMSA Project Office National Astronomical Observatory of Japan 2-21-1 Osawa, Mitaka, Tokyo 181-8588 Japan.

[3]Present address: Sub-mm Telescope Observatory, Steward Observatory, The University of Arizona, Tucson, AZ, 85721.

ABSTRACT

We present HHT observations in the $N = 3 \rightarrow 2$ rotational transition of the CN radical toward selected positions of the Trapezium region and of the molecular Ridge in the Orion molecular cloud. Two of the positions in the Ridge were also observed in the $N = 2 \rightarrow 1$ line of CN and ^{13}CN. The $N = 3 \rightarrow 2$ CN lines have been combined with observations of the $N = 2 \rightarrow 1$ and $N = 1 \rightarrow 0$ transitions of CN, and of the $N = 2 \rightarrow 1$ of ^{13}CN to estimate the physical conditions and CN abundances in the molecular gas. We analyze in detail the excitation of the CN lines and find that the hyperfine ratios of the $N = 3 \rightarrow 2$ line are always close to the Local Thermodynamic Equilibrium (LTE) optically thin values even in the case of optically thick emission. This is due to different excitation temperatures for the different hyperfine lines. From the line intensity ratios between the different CN transitions we derive H_2 densities of $\sim 10^5\,\mathrm{cm}^{-3}$ for the molecular Ridge and of $\sim 3 \times 10^6\,\mathrm{cm}^{-3}$ for the Trapezium region. The CN column densities are one order of magnitude larger in the Ridge than in the Trapezium region, but the CN to H_2 ratio is similar both in the Trapezium and in the Ridge. The combination of the low CN column densities, high H_2 densities and relatively high CN abundances toward the Trapezium region requires that the CN emission arises from a thin layer with a depth along the line of sight of only $\sim 5 \times 10^{15}\,\mathrm{cm}$. This high density thin layer of molecular gas seems to be related with material that confines the rear side of the H II region Orion A. However the molecular layer is not moving as expected from the expansion of the H II region, but it is "static" with respect to the gas in the molecular cloud. We discuss the implication of a high density "static" layer in the evolution of an H II region.

Subject headings: ISM: clouds – ISM: Orion A; Orion clouds – ISM: molecules – Radiolines: ISM

1. Introduction

The dynamical interaction between newly formed massive stars, their H II regions, and the surrounding neutral material has been a topic of great interest. Based on simple ideas, many have argued that H II regions should expand quickly into the ambient molecular cloud, expanding beyond the ultra-compact phase in 10^2–10^3 yr (e.g. Dreher & Welch, 1981, Dreher et al. 1984). It has been recognized that a lifetime paradox exists for ultra-compact H II regions, in that there are far too many given the current birth rate of massive stars (Wood & Churchwell, 1989).

Numerous authors have suggested resolutions for the H II region lifetime paradox (see review of Hollenbach et al. 1994): a) confinement by infalling material (e.g. Reid et al. 1981), b) champagne flows (e.g. Tenorio–Tagle, 1979), c) moving star bow shock (e.g. Van Buren et al. 1990), d) disk photoevaporation model (Hollenbach et al. 1994), and e) mass loaded winds (Dyson et al., 1995; Lizano et al., 1996). These models have been developed to various degrees but all exhibit serious shortcomings when it comes to matching current observational data. De Pree et al. (1995) have suggested a simple resolution for the lifetime paradox. Revisiting the lifetime arguments, but assuming confinement by hot (100 K) and high density ($10^7\,\mathrm{cm}^{-3}$) ambient material, De Pree et al. (1995) find that the ultra-compact H II region phase can persist for $\sim 10^5$ yr.

To study the interfaces between the H II regions and the surrounding material, one must find the appropriate tracers. The usual high density tracers such as CS are not useful

because they are not specific to the interfaces of the H II regions: there are also high column densities of this molecule in hot cores.

From theoretical arguments and observations it is known that the abundances of some molecules are enhanced by UV radiation from the H II region. Based on the results of the Photon Dominated Regions (PDRs) in NGC 2023 and NGC 7023 (Fuente et al. 1993, 1995) and on PDR chemical models (Sternberg and Dalgarno 1995, Jansen et al. 1995), we have selected CN as one of the best tracer of the material at the H II/H_2 boundary layer affected by the UV photons from the OB stars.

Rodríguez–Franco et al. (1998) have used the 30-m telescope to map the $N = 2 \rightarrow 1$ and the $N = 1 \rightarrow 0$ lines of CN towards M 42 and M 43. Modeling the CN emission, Rodríguez–Franco et al. (1998) have produced H_2 density maps in the Orion M 42 and M 43 regions. The CN emission reveals a number of high density ($\sim 10^5\,\mathrm{cm}^{-3}$) bars (north bar, optical bar, molecular filaments, and molecular Ridge) that surround the Trapezium cluster. The CN bars represent the interfaces between the molecular cloud and the major ionization fronts of M 42, confining this H II region in basically all directions except along the line of sight. Surprisingly, the largest H_2 densities, $> 10^6\,\mathrm{cm}^{-3}$ are found towards the Trapezium region where the emission from CO is relatively weak. This CN emission from the Trapezium arises from the thin layer of molecular gas that is related with the material that interacts with the rear ionization fronts of M 42 confining the H II region in this direction. The CN layer is likely to be the remnant of the high density layer ($\sim 10^7\,\mathrm{cm}^{-3}$) that also confined the H II region in the ultra- and hyper-compact phase.

The critical densities to excite the $N = 1 \rightarrow 0$ and $N = 2 \rightarrow 1$ lines of CN are $\sim 10^6\,\mathrm{cm}^{-3}$. Therefore from the analysis of these transitions one cannot constrain the H_2 densities if they are larger than $10^6\,\mathrm{cm}^{-3}$. To estimate the H_2 densities in the Trapezium region one needs to measure a transition with higher Einstein coefficients. In this paper,

we present observations of the CN $N = 3 \rightarrow 2$ transition taken with an angular resolution similar to that of the $N = 1 \rightarrow 0$ line and analyze the new results combined with 30-m data. The new data show that the H_2 densities in the Trapezium layer are $\sim 3 \times 10^6\,\mathrm{cm}^{-3}$.

2. Observations and results

The observations of the $N = 3 \rightarrow 2$ and the $N = 2 \rightarrow 1$ lines of CN, at 340.2 GHz and 226.3 GHz respectively, and the $N = 2 \rightarrow 1$ of ^{13}CN at 217.4 GHz were taken between 27 April and 3 May 1999 and April 2000 with the Heinrich Hertz Telescope (HHT) in Arizona (USA). At the rest frequencies of the $N = 3 \rightarrow 2$ and the $N = 2 \rightarrow 1$, the full width to half power of the telescope was 26″ and 34″ respectively. The pointing was checked by continuum cross scans of Venus. The RMS pointing error was always less than ∼3″. The 345 GHz receiver is a facility instrument consisting of a dual channel superconducting mixer provided by the Max Plank Institut für Radioastronomie (MPIFR). The double sideband receiver noise temperatures were typically ∼150-200 K and ∼100 K for the 345 GHz and 230 GHz receivers respectively. At the elevation of Orion, the single sideband system noise temperature was typically ∼800 to 1400 K for the 345 GHz receiver and ∼ 390 to 760 K for the 230 GHz receiver. The data were calibrated using the chopper wheel method. We have used position switching, with the reference at (−800″, 0″) from the on- source position. We established the final temperature scale by comparisons of our Orion-KL results with the data of Groesbeck et al. (1994) and Schilke et al. (1997) .

For some tunings of the 345 GHz receiver, there is a frequency-dependent variable ratio between the signal and image sidebands with a frequency of ∼500 MHz. To check for the presence of such variability, we shifted each spectrum five times by up to $300\,\mathrm{km\,s}^{-1}$. This also allowed us to measure all the hyperfine components with the narrow band spectrometers, and to search for the presence of intense lines in the image spectrum.

The spectra were analyzed using filter banks and Acoustic Optical Spectrometers (AOS's). The wide band AOS's with a bandwidth of 983 MHz had a resolution of 480 kHz and the narrow band AOS's with a bandwidth of 64 MHz has a resolution of 250 kHz. The $F = 9/2 \rightarrow 7/2$, $F = 7/2 \rightarrow 5/2$, and $F = 7/2 \rightarrow 3/2$ hyperfine components of the $N = 3 \rightarrow 2$, $J = 7/2 \rightarrow 5/2$ multiplet of CN are separated by 790 MHz. This range of frequencies was in the analyzing band of the wide-band AOS's. For the $N = 2 \rightarrow 1$ line of CN the $F = 5/2 \rightarrow 3/2$, $F = 3/2 \rightarrow 5/2$, $F = 3/2 \rightarrow 3/2$, $F = 3/2 \rightarrow 1/2$, $F = 1/2 \rightarrow 3/2$, and $F = 1/2 \rightarrow 1/2$ HF components of the fine $J = 3/2 \rightarrow 3/2$ transition was observed with the 64 MHz narrow band AOS.

The observations were made toward selected positions in the Ridge and in the Trapezium region obtained from the CN $N = 1 \rightarrow 0$ line map of Rodríguez–Franco et al. (1998). Fig. 1 shows superimposed on the CN $N = 1 \rightarrow 0$ map from Rodríguez–Franco et al. (1998) the positions in the Trapezium region (T1. . . T6) and in the molecular Ridge (R1. . . R6) where we took the spectra in the $N = 3 \rightarrow 2$ line of CN. The $N = 2 \rightarrow 1$ line of CN and ^{13}CN were measured toward the positions R4 and R5.

Fig. 2 shows the spectra of the $N = 3 \rightarrow 2$ line toward all the observed positions, and Fig. 3 the $N = 2 \rightarrow 1$ spectra of CN and ^{13}CN towards R4 and R5. Table 1 gives the observational parameters derived from Gaussian fits to the $F = 9/2 \rightarrow 7/2$, $F = 7/2 \rightarrow 5/2$, and $F = 7/2 \rightarrow 3/2$ hyperfine (hereafter HF) components of the $N = 3 \rightarrow 2$, $J = 7/2 \rightarrow 5/2$ multiplet. Table 1 gives also the observed parameters of the $N = 2 \rightarrow 1$ line of CN and ^{13}CN the line towards R4 and R5 (see next section for a discussion).

3. CN line opacities from the hyperfine ratios

Usually one can use the intensity ratio between the fine and HF components of the CN transitions to estimate the optical depth of the lines (see e.g. Rodríguez–Franco et al. 1998). This method is widely used for molecules like NH_3 (Pauls et al. 1983) and gives reliable results when all the HF components have the same excitation temperature. In some cases, like for NH_3 and CN, it is well known that the different HF components might have different excitation temperatures (Gaume et al. 1996). We now discuss the problems associated with the use the HF ratios to estimate the CN line opacities for the submillimeter lines of CN.

The $N = 1 \rightarrow 0$ rotational transition results in 9 HF components grouped in two main fine-structure groups, the $N = 2 \rightarrow 1$ and the $N = 3 \rightarrow 2$ transitions are split in 18 HF lines which are grouped in three fine-structure groups, and the ^{13}CN $N = 2 \rightarrow 1$ line is split into 71 HF components. In the wide band AOS we have observed the two most intense fine structure groups of the $N = 3 \rightarrow 2$ line simultaneously. We have also measured the $J = 3/2 \rightarrow 3/2$ fine structure group in the $N = 2 \rightarrow 1$ line. We have derived the HF ratio for the observed CN lines by fitting a "comb" of Gaussian profiles centered at the frequencies and the relative intensities of the HF components for every CN line. Fig 3 shows the fits of the HF components for the CN and ^{13}CN $N = 2 \rightarrow 1$ line in the two positions of the Ridge. Similar good fits are also obtained for the CN $N = 3 \rightarrow 2$ HF components in Fig. 2. For both the Ridge and the Trapezium positions, we derive a ratio between the $J = 7/2 \rightarrow 5/2$ and the $J = 5/2 \rightarrow 3/2$ fine components of the $N = 3 \rightarrow 2$ line (RF32 hereafter) close to ~ 1.5 (see Table 1), which would indicate optically thin emission. This is surprising in view of the relatively strong CN $N = 3 \rightarrow 2$ lines in the Ridge and the detection of the ^{13}CN $N = 2 \rightarrow 1$ line towards two positions in the Ridge. These facts indicate that the CN lines in the Ridge cannot be optically thin in contrast to the

RF32 indicating optically thin emission. These discrepancies are due to different excitation temperatures for different HF components.

In order to study to what extent the assumption of equal excitation temperature for all the HF components can be applied to the $N = 3 \rightarrow 2$ line to derive the opacities, we have studied the excitation of CN by combining the CN and ^{13}CN line intensities measured in this paper with those measured by Rodríguez–Franco et al. (1998). For this, we have used the model based on the Large Velocity Gradient (LVG) approximation described by Rodríguez–Franco et al. (1998) and a constant kinetic temperature of 80 K (Wilson et al. 2000). In this model only collisional excitation has been considered. The effects of the excitation of the first vibrationally excited levels by infrared radiation at 4.8 microns has been considered negligible for the typical physical conditions in photodissociation regions (Fuente et al. 1995). The data of Rodríguez–Franco et al. (1998) have been smoothed to have the same angular resolution as the HHT CN $N = 3 \rightarrow 2$ data. Figs. 4a and b show the results obtained from the LVG model calculations. Fig. 4a shows the dependence of the H_2 densities (n_{H_2}) with the CN column density (N(CN)) as a function of the intensity of main group of components of the $N = 3 \rightarrow 2$ multiplet, $T_a^*(3 \rightarrow 2)$ (thick line) observed in this paper and the ratio between the intensities of the $N = 3 \rightarrow 2$ and $N = 2 \rightarrow 1$ lines, R31 (dotted lines). In Fig. 4b we plot the H_2 density versus the CN column density as a function of the optical depth of the $N = 3 \rightarrow 2$, $J = 7/2 \rightarrow 5/2$, $F = 9/2 \rightarrow 7/2$ line, $\tau_{\rm m}(3 \rightarrow 2)$, and the ratio between the fine components RF32. Fig. 4b shows that model predicts for a rather wide range of H_2 densities and CN column densities, line intensity ratios around 1.5 (see Table 1). Even for the case of optically thick emission with opacities between 1 and 5 the predicted value of RF32 will be of ~ 1.5. This is clearly the case for the two positions in the Ridge R4 and R5.

In order to fit the ^{13}CN and CN lines simultaneously in the two Ridge positions R4

and R5 where ^{13}CN was observed, ^{13}CN column densities of $\sim 10^{13}\,\mathrm{cm}^{-2}$ are required. Assuming a standard CN/^{13}CN ratio of 89 (Wilson 1999), the CN column density must be close to $\sim 10^{15}\,\mathrm{cm}^{-2}$. For this column density, the HF component of CN $N = 3 \rightarrow 2$ line presented in this paper is optically thick with opacities ≤ 5 (see Fig. 4b) and the expected HF ratio RF32 of ~ 1.5. This indicates, as previously mentioned, that the HF ratio does not necessarily give a measure of the CN line optical depths. This is because the excitation temperature is not the same for all the observed hyperfine components. Since the excitation is mainly collisional, the excitation temperature is expected to be higher in the hyperfine components with higher opacities. In fact, in the simple isothermal case considered in this paper, the LVG model gives $T_{ex} \sim 23\,\mathrm{K}$ and $14\,\mathrm{K}$ for the $J = 5/2 \rightarrow 3/2$ and $J = 7/2 \rightarrow 5/2$ fine components of the $N = 3 \rightarrow 2$ transition respectively. Because of these differences in the excitation temperature, the ratio between the HF structure components remains quite uniform and close to 1.5 for a large range of opacities.

In summary, the HF line intensity ratio of the $N = 3 \rightarrow 2$ CN line does not necessary give a reliable estimate of the line opacity even if the ratios are close to the expected optically thin case. Observations of the ^{13}CN line and/or a number of HF components with a wide range of relative intensities are needed to estimate the opacities of the strongest HF lines of CN.

4. Physical conditions

As shown in Fig. 4a one can use the line intensity ratio of the $N = 3 \rightarrow 2$, and the $N = 1 \rightarrow 0$ lines of CN to derive the H_2 density and the CN column density for the observed position in the Ridge and in the Trapezium once the kinetic temperature is known.

In Table 2 we present the results for the H_2 densities and CN column densities for the

Trapezium and the Ridge for a kinetic temperature of 80 K. These results are basically independent of the assumed kinetic temperatures for kinetic temperatures larger than 25 K (Rodríguez–Franco et al. 1998). For the positions in the Ridge we cannot fit the intensity of the CN $N = 3 \rightarrow 2$ line and the ratio R31 for the optically thin solution. Therefore we have considered the solution for the optically thick case found in the previous section for R4 and R5. For the Trapezium positions, the CN $N = 3 \rightarrow 2$ line is weaker than in the Ridge, and the optically thin solution can explain both, the line intensities and the ratio R31.

The Trapezium and the Ridge regions present very different physical conditions (see Table 2). In the Trapezium region, the densities are between 6×10^5 and $7 \times 10^6\,\mathrm{cm}^{-3}\,\mathrm{cm}^{-3}$ and CN column densities around $4 \times 10^{13}\,\mathrm{cm}^{-2}$. With these physical conditions the opacity of the main hyperfine component of the CN $N = 3 \rightarrow 2$ line is $\tau_m(3 \rightarrow 2) \leq 0.5$ as expected from the hyperfine ratios of the CN $N = 3 \rightarrow 2$ and $N = 1 \rightarrow 0$ lines. For the Ridge we obtain densities between 3×10^4 and $2 \times 10^5\,\mathrm{cm}^{-3}$, CN column densities between 3×10^{14} and $2.5 \times 10^{15}\,\mathrm{cm}^{-2}$, and opacities between 1 and 5. The derived H_2 densities for the Ridge from the CN emission are in good agreement with those derived from HC_3N (Rodríguez−Franco et al. 1992).

In summary, the $N = 3 \rightarrow 2$ CN data confirm the H_2 densities for the Trapezium region, typically of a few $10^6\,\mathrm{cm}^{-3}$. These are larger, on average, by a factor of ~ 10 than those in the molecular Ridge ($0.3 - 2 \times 10^5\,\mathrm{cm}^{-3}$). However, the CN column densities in the Ridge ($\sim 1 \times 10^{15}\,\mathrm{cm}^{-2}$) are larger by more than a factor of 10 than in the Trapezium ($\sim 4 \times 10^{13}\,\mathrm{cm}^{-2}$).

4.1. CN abundances

We have also derived the relative abundance of CN in both regions by combining the CN column densities with the H_2 column density estimated from the ^{13}CO and C^{18}O data of White & Sandell (1995) and Wilson et al. (1986). The H_2 column densities have been derived by using the LVG approximation to model the CO excitation and assuming a ^{13}CO/C^{18}O ratio of 5.6. The results are given in Table 2. We find H_2 column densities of $0.5 - 2.4 \times 10^{22}\,\mathrm{cm}^{-2}$ for the Trapezium region and of $4 - 6 \times 10^{23}\,\mathrm{cm}^{-2}$ for the Ridge. ¿From the H_2 and CN column densities, we estimate the CN/H_2 ratios shown in column 5 of Table 2. The CN abundance ratios in the Trapezium region and molecular Ridge are similar, although there is a systematic trend for the CN abundance to be somewhat larger in the Trapezium (average of 4×10^{-9}) than in the Ridge (average of 10^{-9}).

4.2. Depth along the line of sight of the CN emission

Combining the H_2 densities derived for the multi-transitional analysis of CN with the H_2 column densities derived from ^{13}CO and C^{18}O, we can also estimate the thickness of the molecular gas layer along the line of sight. In column 6 of Table 2 we show the results. We derive a thickness for the Ridge of typically 3×10^{17} cm. This is consistent with the emission arising from spherical condensations with a size of $\sim 5 - 10''$. The thickness of the molecular layer in the Trapezium region is $10 - 100$ times smaller than the thickness of the Ridge. The small thickness of the CN emission toward the Trapezium region makes it very unlikely that this emission arises from condensations with spherical geometry as for the Ridge, since this geometry would require condensations with sizes of only $1''$. To explain the observed CN line intensities one would require a large number of these condensations filling the telescope beam. Since the CN emission is extended we conclude that the CN emission in the Trapezium region arises from a thin, $\sim 5 \times 10^{15}$ cm, layer of dense (few $10^6\,\mathrm{cm}^{-3}$)

molecular gas (hereafter the Trapezium molecular layer).

5. Discussion

Rodríguez–Franco et al. (1998) have discussed in detail the implications of the CN emission in the confinement of the Orion A H II region in the perpendicular direction to the line of sight. The geometry of the Trapezium molecular layer, and the chemistry, with large CN abundance as compared with other molecules like HC_3N, confirms that the CN emission is related with the material which confines the rear side of Orion A. The presence of a layer of material behind the Trapezium confining the Orion A H II region is required to explain the kinematics of the ionized gas (Zuckerman, 1973). The confining material will show the typical multilayer (ionized, neutral atomic and molecular) structure expected when molecular material is exposed to UV radiation (see eg. Hollenbach &Tielen 1997). Fig. 5 shows an sketch of the distribution and kinematics of the ionized and molecular gas towards the Trapezium. A model of the location of the different layers along the line of sight has been obtained by O'Dell et al. 1993). The ionized gas is blueshifted with respect to the neutral molecular gas, indicating that the ionized gas is flowing towards the observer. To prevent the ionized gas from escaping from the H II region in the direction away from the observer, the rear side of the H II region must be confined by a dense layer of gas and dust. This is confirmed by the radial velocities of O I and H I. Both the atomic layer probed by O I and H I and the molecular layer probed by CN show velocities close to 9 km s−1, the ambient cloud velocity, suggesting that this neutral gas forms the front face of the neutral confining cloud (O'Dell et al. 1993; van der Wef & Goss 1989). The CN emission towards the Trapezium has similar radial velocities than that of the warm CO (Howe et al. 1993; Wilson et al. 2000) heated by the UV radiation. As expected for a dense photodissociation region (Sternberg & Dalgarno 1995), both molecular emission arise from

basically the same layer which located close to the principal ionization front (see eg. O'Dell et al. 1993). At the opposite side of the ionization from the dense and warm molecular layer will be surrounding by an envelope of molecular and atomic material (see van der Wef & Goss 1989).

The origin of the thin confining layer in the Trapezium and its present morphology is unclear since the evolution of H II regions is far from understood (see e.g. Churchwell 1990). One would think that the dense thin layer has been built up by material swept by the expansion of the H II region in the last 10^6 yr. In this case the molecular component of the confining material should be expanding. Expanding molecular gas with a velocity of at least $5\,\mathrm{km\,s^{-1}}$ has been observed from the CN emission in the molecular molecular bars (northern bar, optical filament) which are believed to belong to the material that confine the H II region in the direction close to the plane of the sky (Rodríguez−Franco et al. 1998). However, the observe thin CN layer has a radial velocity of $\sim 9\,\mathrm{km\,s^{-1}}$, typical of the molecular gas unperturbed by the effects of the H II region. These arguments point towards the possibility that either the CN Trapezium layer is not related to the material that confines the H II region or to the fact that the evolution of M 42 does not fit the simple picture of an H II region expanding at a velocity of $\sim 15\,\mathrm{km\,s^{-1}}$. The first possibility is unlikely since the UV radiation seems to dominate the chemistry of the thin molecular layer indicating small visual extinction (≤ 4 mag) between the ionizing front and the molecular layer (Rodríguez−Franco et al. 1998). Furthermore, the line widths of the CN are broader than those found for the Ridge, revealing a kinematic interaction between the H II region and the Trapezium molecular layer. If the Trapezium molecular layer is indeed interacting with the H II region, the lack of velocity shifts between CO (from the bulk of the Ridge) and CN from the Trapezium layer indicates that the H II region is not expanding away from the observer.

The Trapezium molecular layer would therefore indicate that the presence of “static” layers not only occurs at the early phases of the evolution of the H II regions as shown by Wood & Churchwell (1989), but also in more evolved objects. Although several suggestions have been made to explain the lifetime, morphology and kinematics of the ultra-compact H II regions (see e.g.Tenorio-Tagle 1979; Reid et al. 1980; Van Buren et al. 1990; Hollenbach et al. 1994; Dyson et al. 1995; Lizano et al. 1996), none of these models adequately explain all the observational facts (Jaffe & Martín−Pintado, 1999). Most of the models developed to explain the lifetime paradox such as the bow shocks, mass-loaded winds and confinement by infalling material predict that the confining material is not “static” with respect to the ambient molecular clouds. The disk evaporated model cannot explain the morphology and kinematics of evolved H II regions such us M 42.

The champagne flow could explain both the kinematics of the ionized gas in M 42 and the presence of the “static” and the expanding molecular layers confining M 42. In the scenario of the champagne model, the massive stars are formed within a molecular cloud with a large density gradient. The H II region confined by material with a density gradient will expand in some directions but depending on the density and temperature of of the surrounding material, can be “static” in other directions. As suggested by De Pree et al. (1995) very dense ($10^7\,\mathrm{cm}^{-3}$), and warm (100 K) molecular material would slow down the expansion of an H II region in the early phases and provide an explanation for the presence of “static” layers in more evolved H II regions. In the case of M 42 the H_2 density gradient is along the line of sight with the larger density in the rear side of the H II region, just where the Trapezium layer is found. In the Trapezium layer the H_2 density is larger than $10^6\,\mathrm{cm}^{-3}$ and the kinetic temperatures are ~ 100 K (Wilson et al. 2000). The CN layer will be in pressure equilibrium with the ionized gas for the typical densities of a few $10^4\,\mathrm{cm}^{-3}$ and the electron temperature of 8000 K measured in M42 (Wilson et al. 1997). The small thickness of the the CN layer, as compared to the Ridge, can also be understood in the

framework of the champagne flow since the gas flowing towards the observer has been photo–evaporated from the confining layer as sketched in Fig. 5. If the ionized material is flowing away from the ionization front at a speed of $\sim 10\,\mathrm{km\,s^{-1}}$ the thin molecular layer will be photo–evaporated in a time scale of $\sim 10^5$ years.

6. Conclusions

We have used the HHT Telescope to carry out observations of the $N = 3 \rightarrow 2$ and new observations of the $N = 2 \rightarrow 1$ lines of CN toward selected positions in the Trapezium region and in the molecular Ridge of the Orion A molecular cloud. The main results are summarized as follow.

1. The hyperfine intensity ratio of just one transition of CN does not give reliable estimate of the optical depth of the lines due to different excitation temperatures for different HF components. The ratios between HF components of the $N = 3 \rightarrow 2$ line can be close to optically thin values even in the case of optically thick emission Observations of several HF groups with very different intensities or/and observations of isotopic substitute of CN are required to derive reliable opacities.

2. Our measurements of $N = 3 \rightarrow 2$ line of CN confirm the presence of a high density (a few $10^6\,\mathrm{cm^{-3}}$) molecular gas toward the Trapezium region with also relatively large CN abundances ($\sim 10^{-9}$). The H_2 density in the Trapezium is a factor of 10 larger than in the Ridge.

3. The high density molecular gas towards the Trapezium is located in a thin layer ($\sim 5 \times 10^{15}$ cm). This thin molecular layer is related with the material that confines the far side of the H II region in the Trapezium region, and it is “static” with respect to the molecular cloud.

4. The kinematics of the ionized gas and the small thickness of the Trapezium layer can be understood in the framework of the champagne flows. The "static" molecular layer is in equilibrium with the H II region suggesting that evolved H II regions are not expanding in all directions as occurs for UC H II regions.

REFERENCES

De Pree, C.G., Rodríguez, L.F., Goss, W.M., 1995, Rev. Mex. A.A 31, 39.

Churchwell, E., 1990, A&AR 2, 79.

Dreher, J.W., Welch, W.J., 1981, ApJ 245, 857.

Dreher, J.W., Johnston, K.J., Welch, W.J., Walker, R.C., 1984, ApJ 283, 632.

Dyson, J.E., Williams, R.J.R., Redman, M.P., 1995, MNRAS 277, 700.

Fuente, A., Martín–Pintado, J., Bachiller, R., Cernicharo, J., 1993, A&A 276, 473.

Fuente, A., Martín–Pintado, J., Gaume, R., 1995, ApJLetters 442, L33.

Gaume, R.A.. Wilson, T.L., Johnston, K.J., 1996 ApJ 457, L47.

Groesbeck, T.D., Phillips, T.G., Blake, G.A., 1994, ApJS 94, 147.

Hollenbach, D., Johnstone, D., Lizano, S., Shu, F., 1994, ApJ 428, 654.

Hollenbach, Tielens, A. 1997 ARA&A 35, 179.

Howe, J.E., Jaffe, D.T., Grossman, E.N., Wall, W.F., Mangum, J.G., Stacey, G.J., 1993, ApJ 410, 179.

Jansen, D.J., Spaans, M., Hogerheijde, M.R., van Dishoeck, E.F., 1995, A&A 303 541.

Lizano, S., Cantó, J., Garay, G., Hollenbach, D.J., 1996, ApJ 468, 739.

Luhman, M.L., Jaffe, D.T., Keller, L.D., Soojong Pak, 1994, ApJLet 436, L185.

Jaffe, D.T., Martín–Pintado, J., 1999, ApJ 520, 162.

O'Dell, C.R., Valk, J.H., Wen, Z., Meyer, D.M., 1993, ApJ 403, 678.

Pauls, A., Wilson, T.L., Bieging, J.H., Martin, R.N., 1983 A&A 124, 23.

Reid, M.J., Haschick, A.D., Burke, B.F., Moran, J.M., Johnston, K.J., Swenson, G.W. Jr., 1980, ApJ 239, 89.

Rodríguez–Franco, A., Martín–Pintado, J., Gómez–González, J., Planesas, P., 1992 A&A 264, 592.

Rodríguez–Franco, A., Martín–Pintado J., Fuente, A, 1998, A&A 329, 197

Schilke, P., Groesbeck, T.D., Blake, G.A., Phillips, T. G., 1997 ApJS 108, 301.

Sternberg, A., Dalgarno, A., 1995, ApJss 99, 565.

Tenorio–Tagle, G., 1979, A&A 71, 59.

Van Buren, D., Mac Low, M. M., Wood, D.O.S., Churchwell, E., 1990, ApJ 353, 570.

van der Werf, P.P., Goss, W.M., 1989, A&A 224, 209.

White G.J., Sandell G., 1995, A&A 299, 179.

Wilson, T.L., Serabyn, E., Henkel, C., Walmsley, C.M., 1986, A&A 158, L1.

Wilson, T.L., Filges, L., Codella, C., Reich, W., Reich, P., 1997, A&A 327, 1177.

Wilson, T.L., 1999, Rep. Prog. Phys 62, 143.

Wilson, T.L., Muders, D., Kramer, C., Henkel, C., 2000, ApJ, submited.

Wood, D.O.S., Churchwell, E., 1989, ApJSupp 69, 831.

Zuckerman, B., 1973, ApJ 183, 863.

This manuscript was prepared with the AAS LaTeX macros v5.0.

Fig. 1.— Location of the positions observed in the CN $N = 3 \rightarrow 2$ line in the Trapezium region (T1. . . T6) and in the molecular Ridge (R1. . . R6) superposed on the spatial distribution of the CN $N = 1 \rightarrow 0$ line integrated intensity between 0 and $14\,\mathrm{km\,s^{-1}}$ towards Orion A from Rodríguez–Franco et al. (1998). The offsets are relative to the position of IRc2 (α(1950)=5$^{\mathrm{h}}$ 32$^{\mathrm{m}}$ 47.0$^{\mathrm{s}}$, δ(1950)=–5$^{\mathrm{o}}$ 24$'$ 20.6$''$). First contour level is $2\,\mathrm{K\,km\,s^{-1}}$ and the interval between contours is $3.5\,\mathrm{K\,km\,s^{-1}}$.

Fig. 2.— Spectra (solid line) and fits (grey line) of the CN $N = 3 \rightarrow 2$ line taken towards the Trapezium region (left panels) and towards the molecular Ridge (right panels). The position (offsets in arc-seconds respect the position of IRc2) where the spectra were taken is noted in the upper right corner of each box. In the upper left corner appear the nomenclature used in Fig. 1.

Fig. 3.— Spectra (solid line) and fits (grey line) of the CN $N = 2 \rightarrow 1$ and ^{13}CN $N = 2 \rightarrow 1$ line taken towards two positions in the Ridge.

Fig. 4.— LVG diagrams for a kinetic temperature of 80 K. **a)** Solid lines represent the intensity in Kelvin of the main fine group component of the $N = 3 \rightarrow 2$ multiplet. Dotted lines, labeled R31, represent the ratio between the intensity of the main fine group of the $N = 3 \rightarrow 2$ multiplet and the intensity of the main fine group of the $N = 1 \rightarrow 0$ multiplet. **b)** Solid lines represent the opacity of the main HF component of the fine group component of the $N = 3 \rightarrow 2$ multiplet. Dotted lines represent the ratio between the intensity of the $J = 7/2 \rightarrow 5/2$ and $J = 5/2 \rightarrow 3/2$ fine groups of the $N = 3 \rightarrow 2$ multiplet

Fig. 5.— Sketch of the of the distribution and kinematics of the ionized and molecular gas towards the Trapezium. The sizes of the different layers are not represented with the same scale and they have chosen to show the different components.

Table 1. Observational parameters of the CN emission.

Position ($''$,$''$)	$T_a^*(32)$[a] (K)	v_{LSR}[a] ($km\,s^{-1}$)	Δv[a] ($km\,s^{-1}$)	$T_a^*(21)$[b] (K)	$T_a^*(^{13}21)$[b] (K)	$T_a^*(10)$[c] (K)	RF(32)
T1 (60,−24)	0.9	9.5	5.9			0.4	1.6
T2 (108,24)	0.6	9.9	3.8			< 0.4	1.4
T3 (180,−24)	2.1	10.4	3.2			1.2	1.3
T4 (48,−48)	1.1	9.2	4.1			1.3	1.6
T5 (96,−72)	0.3	9.7	5.3			< 0.6	0.9
T6 (38,−84)	2.6	8.8	3.9			0.6	1.3
R1 (41,186)	5.4	9.6	2.5			10.9	1.3
R2 (0,113)	2.8	9.2	2.4			12.0	1.6
R3 (−41,15)	3.1	7.8	3.2			4.9	1.5
R4 (−41,−41)	4.7	7.6	3.6	0.46	0.12	7.5	1.3
R5 (−31,−113)	4.7	7.2	3.7	0.43	0.13	9.0	1.5
R6 (−21,−247)	3.1	8.6	1.7			6.2	1.4

[a]Fits to the $F = 9/2 \rightarrow 7/2$, $F = 7/2 \rightarrow 5/2$, and $F = 7/2 \rightarrow 3/2$ hyperfine components of the $N = 3 \rightarrow 2$, $J = 7/2 \rightarrow 5/2$ multiplet

[b]Fits to the $F = 3/2 \rightarrow 3/2$ hyperfine component of the $N = 2 \rightarrow 1$, $J = 3/2 \rightarrow 3/2$ multiplet

[c]Fits to the $F = 5/2 \rightarrow 3/2$ hyperfine component of the $N = 1 \rightarrow 0$, $J = 3/2 \rightarrow 1/2$ multiplet (from Rodríguez−Franco et al. 1998)

Table 2. Derived parameters of the CN emission.

Position	N(CN)	$N(H_2)$	n_{H_2}	χ(CN)	depth[e]	$N(^{13}CN)$
($''$,$''$)	($\times 10^{13}$ cm^{-2})	($\times 10^{22}$ cm^{-2})	($\times 10^{5}$ cm^{-3})	($\times 10^{-9}$)	($\times 10^{16}$ cm)	($\times 10^{13}$ cm^{-2})
T1 (60,−24)	8.0	2.59[a]	6	3.1	4.31	
T2 (108,24)	2.2	0.86[a]	12.5	2.5	0.69	
T3 (180,−24)	3.0	0.86[a]	50	3.5	0.17	
T4 (48,−48)	3.3	3.46[a]	6	0.9	5.77	
T5 (96,−72)	1.7	0.43[a]	10	3.9	0.43	
T6 (38,-84)	4.3	0.86[a]	70	4.9	0.12	
R1 (41,186)	245		1			
R2 (0,113)	240	6.06[b]	0.31	39	195	
R3 (−41,15)	30	10.4[c]	2	2.8	52.0	
R4 (−41,−41)	97	12.1[c]	1	8.0	121	1.3
R5 (−31,−113)	75	12.1[c]	2	6.2	60.7	1.0
R6 (−21,−247)	90	11.2[b]	0.7	8.0	160	

[a]From ^{13}CO data (White & Sandell, 1995)

[b]From ^{13}CO and C^{18}O data (White & Sandell, 1995)

[c]From C^{18}O data (White & Sandell, 1995)

[d]Assumed n_{H_2}

[e]From the N_{H_2} in column 3 and the n_{H_2} in column 4

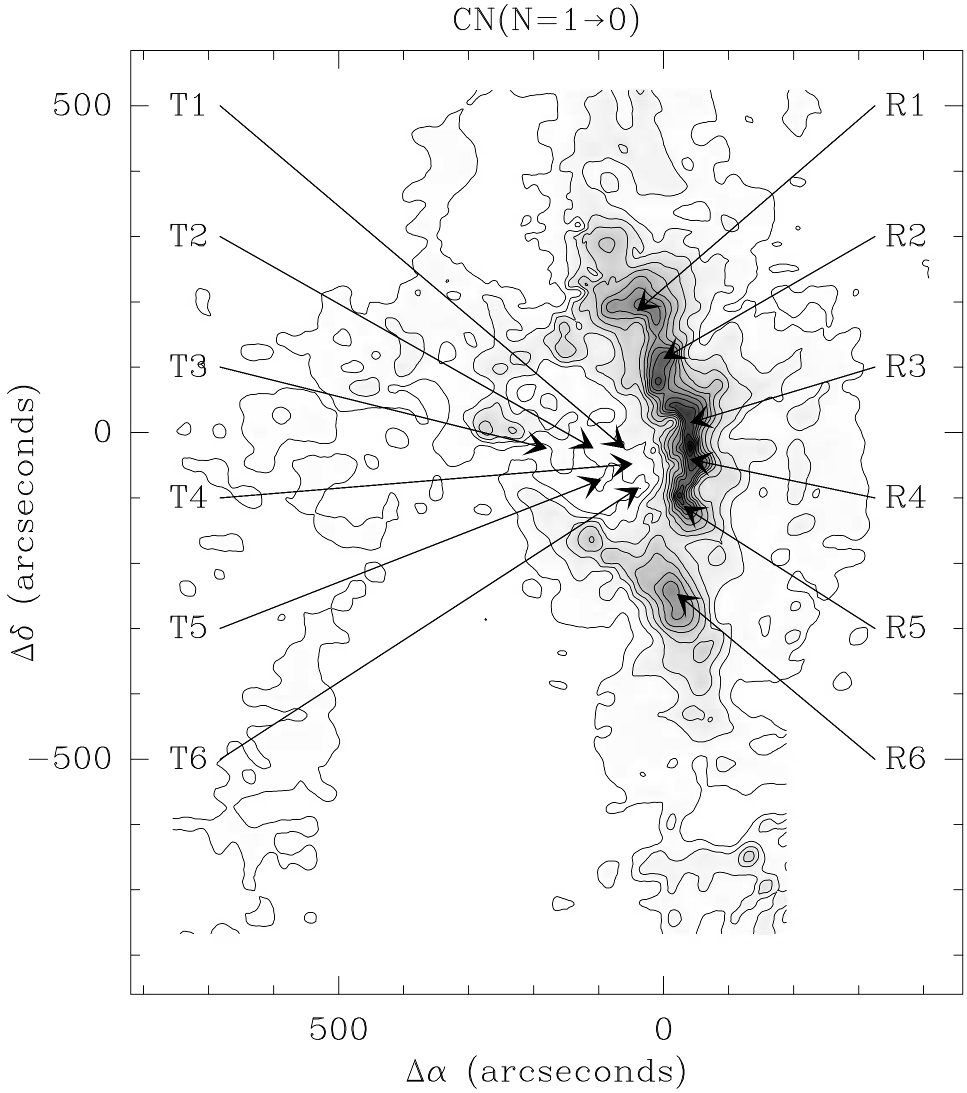
CN(N=1→0)
T1
T2
T3
T4
T5
T6
R1
R2
R3
R4
R5
R6
500
0
−500
500
0
Δδ (arcseconds)
Δα (arcseconds)

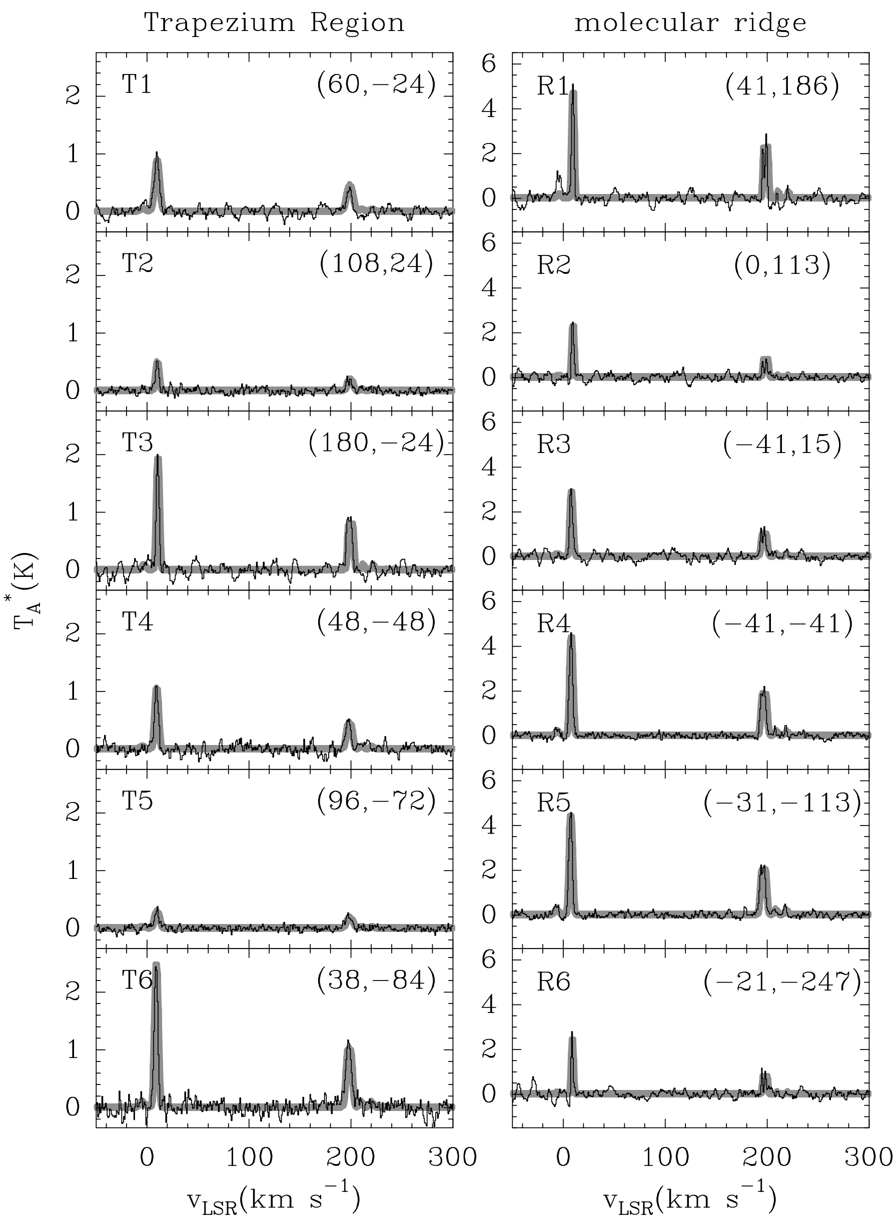

Trapezium Region
molecular ridge
T1
(60,−24)
T2
(108,24)
T3
(180,−24)
T4
(48,−48)
T5
(96,−72)
T6
(38,−84)
R1
(41,186)
R2
(0,113)
R3
(−41,15)
R4
(−41,−41)
R5
(−31,−113)
R6
(−21,−247)
T_A^*(K)
v_{LSR}(km s^{-1})

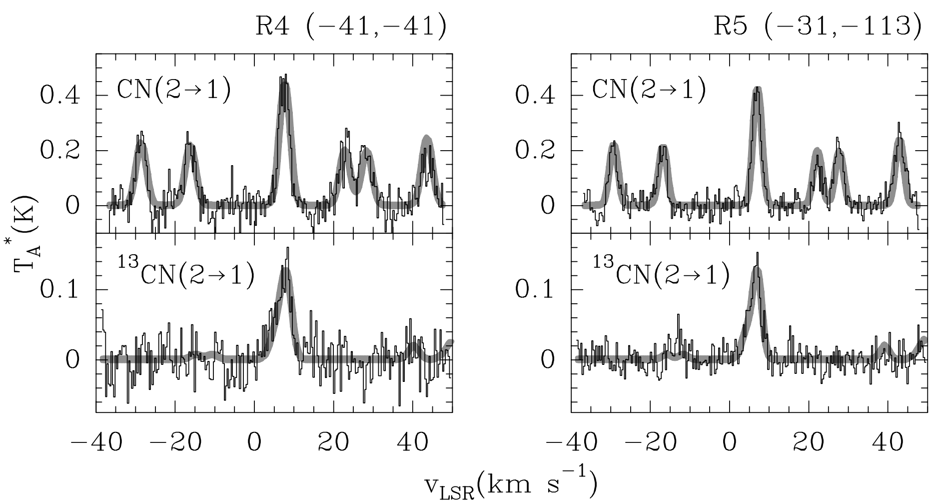
R4 (−41,−41)
R5 (−31,−113)
CN(2→1)
CN(2→1)
13CN(2→1)
13CN(2→1)
T*A(K)
vLSR(km s−1)
0.4
0.2
0
0.1
0
−40 −20 0 20 40

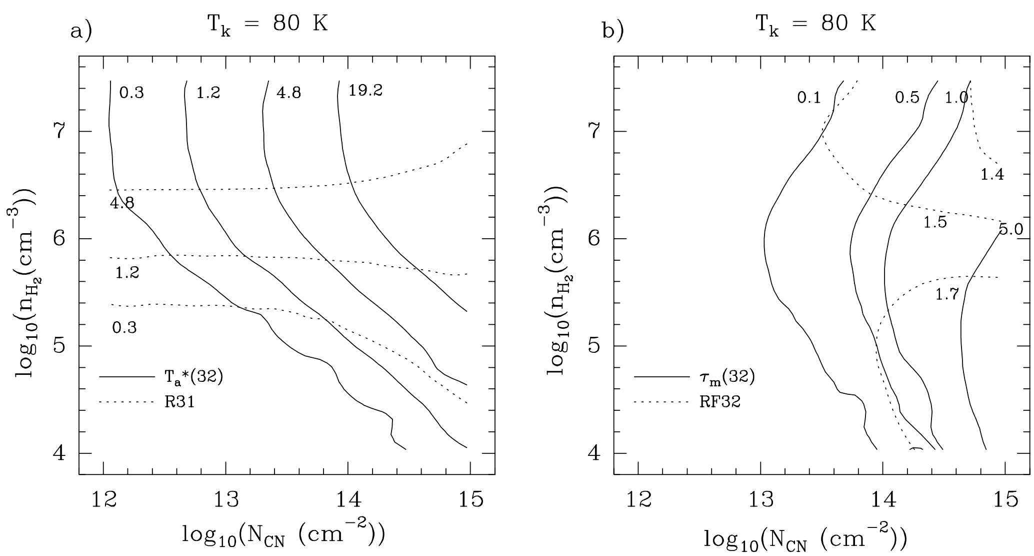
a)
T_k = 80 K
0.3
1.2
4.8
19.2
4.8
1.2
0.3
T_a*(32)
R31
$\log_{10}(n_{H_2}(cm^{-3}))$
$\log_{10}(N_{CN}\ (cm^{-2}))$
b)
T_k = 80 K
0.1
0.5
1.0
1.4
1.5
5.0
1.7
$\tau_m(32)$
RF32
$\log_{10}(n_{H_2}(cm^{-3}))$
$\log_{10}(N_{CN}\ (cm^{-2}))$

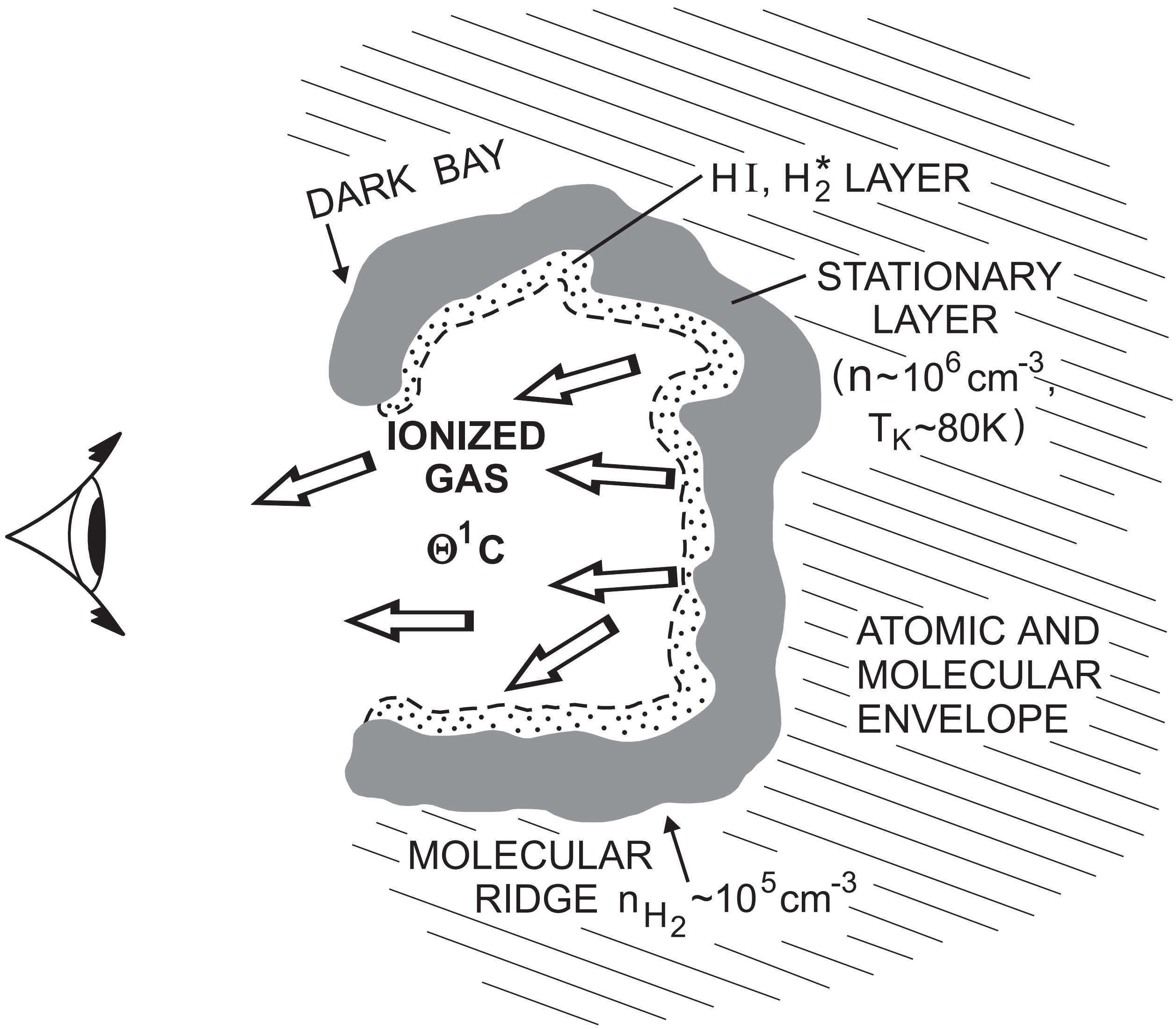
DARK BAY
H I, H_2^* LAYER
STATIONARY LAYER
(n~10^6 cm^{-3}, T_K~80K)
IONIZED GAS
Θ^1C
ATOMIC AND MOLECULAR ENVELOPE
MOLECULAR RIDGE n_{H_2}~10^5 cm^{-3}